

Inelastic neutron scattering and lattice dynamics of NaNbO_3 and $\text{Sr}_{0.70}\text{Ca}_{0.30}\text{TiO}_3$

S K MISHRA^{1,*}, R MITTAL^{1,2}, N CHOUDHURY¹, S L CHAPLOT¹ and
D PANDEY³

¹Solid State Physics Division, Bhabha Atomic Research Centre,
Mumbai 400 085, India

²Forschungszentrum Jülich GmbH, Jülich Centre For Neutron Science,
C/O TU München, Lichtenbergstr 1, 85747 Garching, Germany

³School of Materials Science and Technology, Institute of Technology,
Banaras Hindu University, Varanasi 210 005, India

*Corresponding author. E-mail: skmsspd@barc.gov.in

Abstract. NaNbO_3 and $(\text{Sr,Ca})\text{TiO}_3$ exhibit an unusual complex sequence of temperature- and pressure-driven structural phase transitions. We have carried out lattice dynamical studies to understand the phonon modes responsible for these phase transitions. Inelastic neutron scattering measurements using powder samples were carried out at the Dhruva reactor, which provide the phonon density of states. Lattice dynamical models have been developed for SrTiO_3 and CaTiO_3 which have been fruitfully employed to study the phonon spectra and vibrational properties of the solid solution $(\text{Sr,Ca})\text{TiO}_3$.

Keywords. Lattice dynamics; inelastic neutron scattering; ferroelectrics; antiferroelectric; NaNbO_3 ; SrTiO_3 .

PACS Nos 63.20.D; 77.80.-e; 78.70.Nx

1. Introduction

NaNbO_3 has an antiferroelectric structure at room temperature and finds important technological applications [1–3]. It exhibits an unusual complex sequence of temperature- and pressure-driven structural phase transitions which are associated with zone centre and zone boundary phonons. Recently, we have employed systematic neutron diffraction measurements as a function of temperature ($T=12\text{--}350$ K) to study the low temperature structures and to understand the phase transitions of NaNbO_3 [3]. Our studies present unambiguous evidence for the presence of the ferroelectric $R3c$ phase of NaNbO_3 coexisting with an antiferroelectric phase $Pbcm$) over a wide range of temperatures. The coexisting phases and reported anomalous smearing of the dielectric response akin to dipole glasses and relaxors observed in the same temperature range are consistent with competing ferroelectric and antiferroelectric interactions in NaNbO_3 .

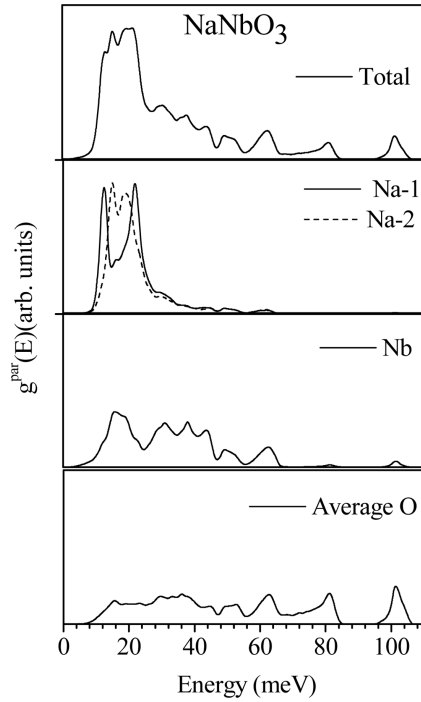


Figure 1. The calculated partial phonon density of states for various atoms in NaNbO_3 . Atoms Na-1 and Na-2 occupy $4c$ and $4d$ Wyckoff position, respectively. For oxygen atoms (which occupy four different crystallographic sites), average partial density of states are plotted.

Similar competing interactions are also observed in solid solution of SrTiO_3 and CaTiO_3 ($\text{Sr}_{1-x}\text{Ca}_x\text{TiO}_3$: SCT) [4]. $\text{Sr}_{1-x}\text{Ca}_x\text{TiO}_3$ exhibits interesting phase transitions from quantum paraelectric, ferroelectric, relaxor ferroelectric to antiferroelectric as a function of temperature and compositions. These phase transitions are driven by zone centre (ferrodistortive) and zone boundary (antiferrodistortive) phonon instabilities. Theoretical lattice dynamics studies are important tools for the analysis of inelastic neutron scattering spectra and help identify the phonon modes that are responsible for these transitions. Inelastic neutron scattering studies using polycrystalline samples have been employed to measure the phonon density of states of NaNbO_3 and $(\text{Sr}_{0.70}\text{Ca}_{0.30})\text{TiO}_3$. We have developed shell model interatomic potentials for NaNbO_3 . Interatomic potentials for the end members SrTiO_3 and CaTiO_3 have been fruitfully employed to study the lattice dynamics of the solid solution $(\text{Sr}_{0.70}\text{Ca}_{0.30})\text{TiO}_3$ (SCT30).

2. Experiment and calculation

The phonon density of states measurements in the energy range of 10–120 meV were carried out for NaNbO_3 and SCT30 using a medium-resolution triple axis spectrometer at Dhruva reactor at Trombay. Polycrystalline sample of about 100 g of NaNbO_3 or 30 g of SCT30 was placed in a thin aluminum container for neutron measurements. The incident energy was varied using a copper (111) monochromator. The phonon spectra in the range of 10–120 meV were measured using a

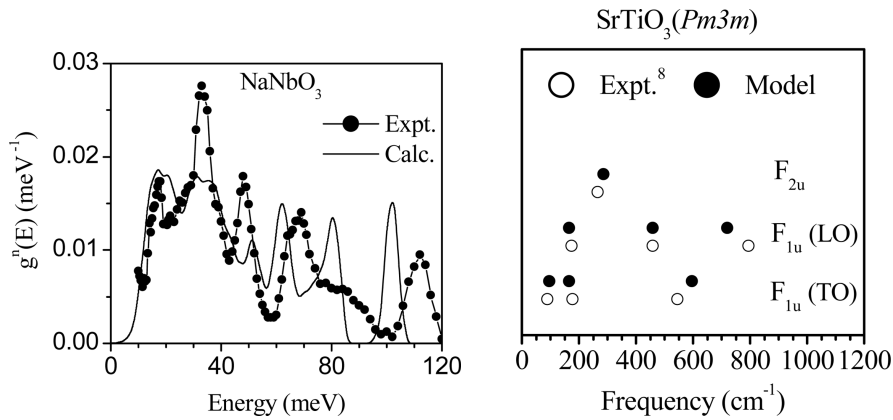


Figure 2. The comparison of the measured (solid circles) and calculated (solid line) phonon density of states of NaNbO_3 .

Figure 3. Comparison between experimentally obtained Raman and infra-red data [8] and the calculated values for SrTiO_3 .

Be filter as an analyzer. Several inelastic runs were recorded with fixed scattering angles between 90° and 110° . All the measurements were made in the energy loss mode.

Transferable interatomic potential models have been developed for computing various thermodynamical properties and analysis of inelastic neutron scattering data in the various phases of NaNbO_3 and SCT30 . The parameters of the potential satisfy the conditions of static and dynamic equilibrium. The polarizability of the oxygen atoms is introduced in the framework of the shell model [5]. The phonon frequencies in the entire Brillouin zone have been calculated using the current version of the program DISPR [6] developed at Trombay. Lattice constants, zone centre phonon frequencies and elastic constants have been fitted to available experimental values.

3. Results and discussion

The calculated long wavelength Raman and infra-red modes for NaNbO_3 show a fair agreement with the experimental data available in the literature. The average deviation between the calculations and the experimental data is about 10%. The calculated partial density of states in the antiferroelectric phase of NaNbO_3 is shown in figure 1. The computed partial density of states reveal that Na contributes in the 0–40 meV range, while Nb and O contribute in the 0–60 meV and the entire spectral ranges of 0–120 meV, respectively. The experimental one-phonon spectra (figure 2) are obtained by subtracting the multiphonon contribution calculated using the Sjolander formalism [7]. The comparison between the experimental and calculated one-phonon neutron-weighted phonon density of states show that their agreement is overall satisfactory.

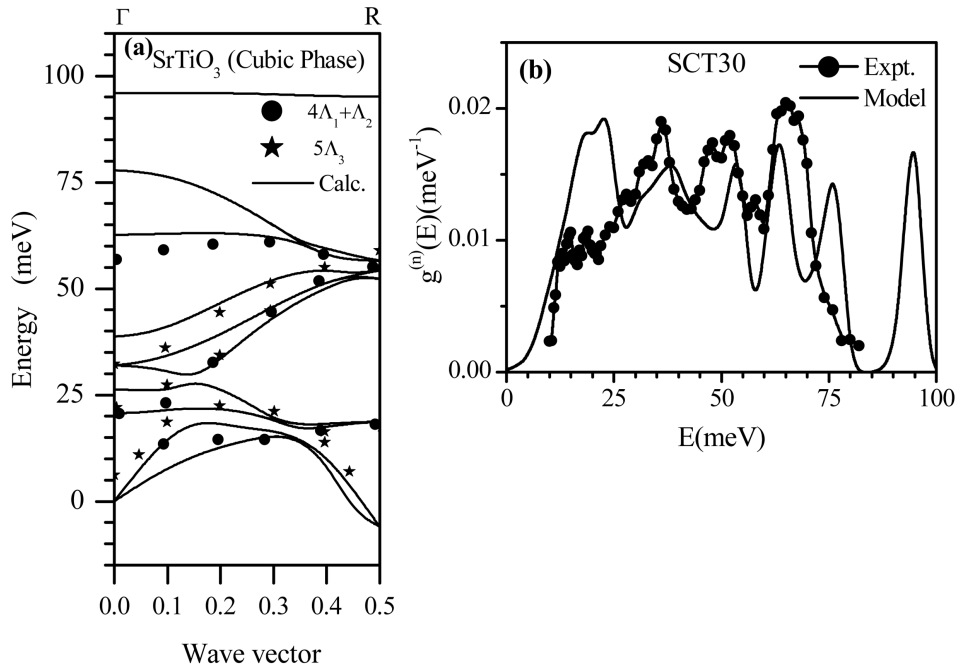


Figure 4. (a) The comparison of the calculated phonon dispersion relation for cubic SrTiO₃ along [111] direction with reported inelastic neutron scattering data (symbol, [9]). (b) Comparison of the experimental (symbols; data upto 80 meV only) and calculated (full line) phonon density of states of SCT30.

In order to carry out lattice dynamical calculations for SCT30, we have first developed a shell model for the end members, i.e. SrTiO₃ and CaTiO₃. Further, we have extended our model for calculations of SCT30. The calculated long wavelength Raman and infra-red modes for SrTiO₃ show (figure 3) a fair agreement with the experimental data [8] available in the literature. The average deviation of our calculations from the experimental data is about <10%. Figure 4 shows the calculated phonon dispersion relations in cubic phase of SrTiO₃ compared with experimental $T = 90$ K inelastic neutron data [9]. Our calculations are in agreement with the neutron data and reported *ab initio* calculations [10].

Modelling the lattice dynamics of disordered system SCT30 was carried out in the virtual-crystal approximation using ordered 20 and 40 atom supercells having tetragonal and orthorhombic symmetry. Calculations were done by introducing virtual atoms Sr/Ca with suitable weighted average values, the mass and also the neutron scattering length. The effects from random disorder were studied using large 540 atom supercells with randomly disordered sites which suggest that introducing disorder in SrTiO₃ by doping Ca²⁺ at Sr²⁺ site mainly influences the low energy modes only [11].

The comparison between the experimental and calculated one-phonon neutron-weighted phonon density of states of SCT30 show that their agreement is overall

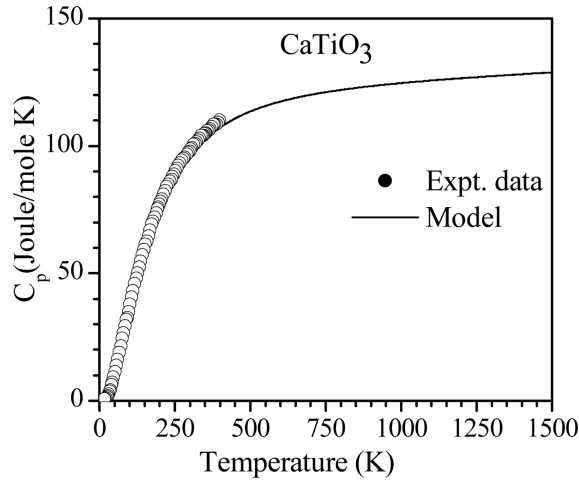


Figure 5. The comparison of the calculated and experimental [12] specific heat for CaTiO_3 .

satisfactory (figure 4b). The calculated partial density of states in the cubic phase of SrTiO_3 , orthorhombic phases of CaTiO_3 and SCT30 show that oxygen atoms in these compounds contribute in the whole energy region up to 103 meV, while Ti atoms mainly contribute up to 65 meV. The vibrations due to Sr atom extend up to 20 meV in SrTiO_3 . Due to lighter mass of Ca in comparison to Sr, the contribution from the Ca atoms extends to higher energies (50 meV) in CaTiO_3 . Above 60 meV, the contributions are mainly due to Ti–O stretching modes. In addition to this, the band gap around 80 meV is largest for SrTiO_3 and decreases with increasing Ca^{2+} .

We have used the shell model for CaTiO_3 to compute various thermodynamic properties (figure 5) like the specific heat and thermal expansion. The computed specific heat of CaTiO_3 is in good agreement (figure 5) with available experimental data [12].

4. Conclusion

We have developed a lattice dynamical model for NaNbO_3 , SrTiO_3 , CaTiO_3 and SCT30 and validated it by our inelastic neutron scattering data and various other experimental data from the literature. The calculations provide a microscopic understanding of the phonon spectra and thermodynamic properties of these technologically important materials.

References

- [1] M E Lines and A M Glass, *Principles and application of ferroelectrics and related materials* (Clarendon, Oxford, 1977)

- Xu Yuhuan, *Ferroelectric materials and their applications* (Elsevier Science, North-Holland, 1991)
- [2] Y Saito *et al*, *Nature (London)* **423**, 84 (2004)
E Cross, *Nature (London)* **432**, 24 (2004)
- [3] S K Mishra *et al*, *Phys. Rev.* **B76**, 024110 (2007) and references therein
- [4] R Ranjan, D Pandey and N P Lalla, *Phys. Rev. Lett.* **84**, 3726 (2000)
S K Mishra, *Studies on structures and phase transitions in [Sr,Ca]TiO₃ ceramics*, Ph.D. Thesis (Banaras Hindu University, 2004) and references therein
- [5] S L Chaplot *et al*, *Eur. J. Mineral.* **14**, 291 (2002)
- [6] S L Chaplot (unpublished)
- [7] A Sjolander, *Arkiv fur Fysik* **14**, 315 (1958)
- [8] W Taylor and A F Murray, *Solid State Commun.* **31**, 937 (1979)
R A Cowley, *Phys. Rev.* **134**, A981 (1964)
A S Barker and M Tinkham, *Phys. Rev.* **125**, 1527 (1962)
W G Spitzer, R C Miller, D A Kleinman and L E Howarth, *Phys. Rev.* **126**, 1710 (1960)
- [9] W G Stirling, *J. Phys.* **C5**, 2711 (1972)
- [10] N Choudhury *et al*, *Phys. Rev.* **B77**, 134111 (2008)
N Sai and D Vanderbilt, *Phys. Rev.* **B62**, 13942 (2000)
C Lasota *et al*, *Ferroelectrics* **194**, 109 (1997)
- [11] S K Mishra *et al* (unpublished)
- [12] Brian F Woodfield *et al*, *J. Chem. Thermodyn.* **31**, 1573 (1999)
C J Shomate *et al*, *J. Am. Chem. Soc.* **68**, 964 (1946)